# Hybrid/mixed Finite Element Analysis of Circular Plate Bending Based on Reissner–Mindlin Theory

Mei Duan***, Yutaka Miyamoto*, Shoji Iwasaki**, Hideaki Deto**
Dept. of Civil and Environmental Engineering, Iwate University, Ueda 4–3–5, Morioka 020,Japan

Professor*, Assistant Professor**, Ph.D. Candidate***

The formulation of hybrid/mixed finite element method (HMFEM) is derived based on Reissner–Mindlin theory. A non–axisymmetric plate bending element of HMFEM under polar coordinate is presented. Some numerical results show that the presented method is valid for circular plate bending problem. The comparisons of solutions demonstrate that HMFEM greatly improves the precision of solutions compared to that of displacement finite element method (DFEM). The presented method may be applied to solve moderately thick/thin circular plate bending problems under all applied load conditions.

*Key Words: Circular plate, hybrid/mixed method, finite element method*

## 1.Introduction

The bending of circular plates is of great interest to the engineering field. Such plate systems can be found in many engineering applications, ranging from more conventional civil engineering and mechanical engineering to aerospace engineering. Most research in the field of plate bending was based on DFEM. However, it is difficult for DFEM to achieve satisfied solutions, even if reduced integration technique is used in the analyses of plate and shell. It is well known that solutions of plate and shell analyses were greatly improved since hybrid finite element method, which is the initial version of HMFEM, was presented by Professor Pian of Massachusetts Institute of Technology in 1964 [1]. During the last thirty years, HMFEM has been well developed, and a good historical survey of HMFEM has been given by Professor Pian in 1996 [2]. Based on papers published regarding the plate bending problems of HMFEM, the authors developed a new HMFEM model based on Reissner–Mindlin plate theory of plate bending [3]. Although the bending of circular plates under rectangular Cartesian coordinate system has been substantially studied, there have been few investigations on circular plate under polar coordinate system with non–symmetry loads. This is because the problems of polar coordinate system are often changed into a rectangular Cartesian system to solve their solutions. More errors in this case have often been made and ignored because of the approximation of solution domain, as shown in Fig.1, so a high amount of elements are necessary in order to achieve satisfactory solutions.

This paper is concerned with an analysis of the moderately thick/thin circular plate bending in polar coordinate. Non–symmetric load is considered.

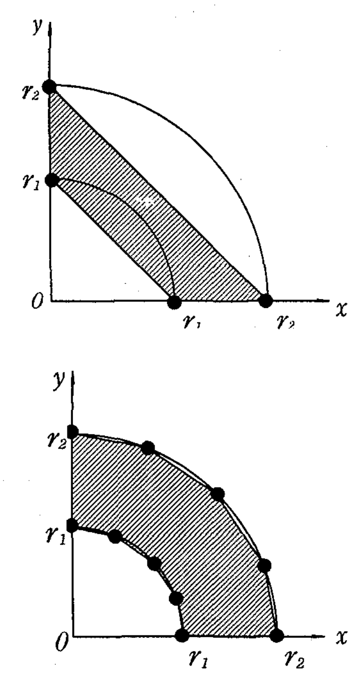


Fig.1 Approximation of solution domain under Cartesian coordinate system

Extending the study by Duan et al.(1995) [4], in this paper, the formulation of HMFEM for plate under the polar coordinate system is derived based on the Reissner–Mindlin plate theory [5–6]. Hybrid/mixed finite element under polar coordinate system is given. Numerical calculations are carried out to investigate the effectiveness of the presented method. The bending behavior of moderately thick/thin plate is investigated and numerical results for plate bending are compared with theoretical solutions and the other numerical methods.

## 2. Theoretical Formulation

Using the geometric mapping relations, as follows:

$$\begin{cases} r=\dfrac{r_1+r_2}{2}+\dfrac{r_2-r_1}{2}\eta \\ \theta=\dfrac{\theta_1+\theta_2}{2}+\dfrac{\theta_1-\theta_2}{2}\xi \end{cases} \quad (\theta_1 \neq \theta_2, \quad r_1 \neq r_2) \tag{1}$$

in which $(r, \theta)$, $(\xi, \eta)$ is polar coordinate, local Cartesian coordinate, respectively, two elements under different plane coordinate system can transform each other, as shown in Fig.2.

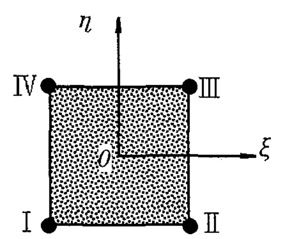


*(a) Local Cartesian coordinate system*

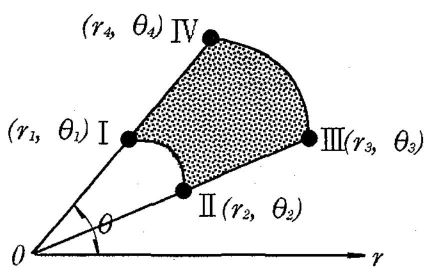


*(b) Polar coordinate system*

Fig.2 Coordinate system of element

For the bending analysis of Reissner−Mindlin plate with uniform thickness, the governing differential equation in terms of displacement under polar coordinate is given, as follows.

$$\Delta^2 w=\frac{p}{D}-\mu\Delta p \tag{2}$$

with $D=\dfrac{Et^3}{12(1-\nu^2)}$ , $\Delta=\dfrac{\partial^2}{\partial r^2}+\dfrac{1}{r}\dfrac{\partial}{\partial r}+\dfrac{1}{r^2}\dfrac{\partial^2}{\partial \theta^2}$

where $w$ is the out−of−plane displacement, $p$ is the load on the plate surface, $E$, $t$ , $\nu$ is Young's modulus, the thickness of the plate and Poisson's ratio, respectively. $\mu=\dfrac{h^2}{10D}\dfrac{2-\nu}{1-\nu}\Delta p$ , $\mu=\dfrac{h^2}{5D(1-\nu)}\Delta p$ indicate Reissner theory and Mindlin theory, respectively.

Let displacement $\boldsymbol{u}$, stress $\boldsymbol{\sigma}$, and strain $\boldsymbol{\varepsilon}$ under polar coordinate system, as follows:

$$\boldsymbol{u}=\begin{Bmatrix} w \\ \psi_r \\ \psi_\theta \end{Bmatrix}=\begin{Bmatrix} w \\ \dfrac{\partial w}{r\partial\theta}-\gamma_{\theta z} \\ -\dfrac{\partial w}{\partial r}+\gamma_{rz} \end{Bmatrix}, \quad \boldsymbol{\sigma}=\begin{Bmatrix} \boldsymbol{M} \\ \boldsymbol{Q} \end{Bmatrix}=\begin{Bmatrix} M_r \\ M_\theta \\ M_{r\theta} \\ Q_r \\ Q_\theta \end{Bmatrix}, \tag{3}$$

$$\boldsymbol{\varepsilon}=\begin{Bmatrix} \boldsymbol{\varepsilon}_f \\ \boldsymbol{\varepsilon}_s \end{Bmatrix}=\begin{Bmatrix} \boldsymbol{D}_f \\ \boldsymbol{D}_s \end{Bmatrix}\boldsymbol{u}$$

in which $\psi_r$ and $\psi_\theta$ are rotation displacements about polar coordinate $r$ and $\theta$, respectively, $\gamma_{\theta z}$ and $\gamma_{rz}$ are average shear strains, $M_r$, $M_\theta$ and $M_{r\theta}$ are the bending and twisting moments, $Q_r$ and $Q_\theta$ are the transverse shear forces, $\boldsymbol{\varepsilon}_f$ and $\boldsymbol{\varepsilon}_s$ are the bending strain and the transverse shear strain, respectively.

$$\boldsymbol{D}_f=\begin{bmatrix} 0 & 0 & \dfrac{\partial}{\partial r} \\ 0 & -\dfrac{\partial}{r\partial\theta} & 0 \\ 0 & -\dfrac{\partial}{\partial r} & \dfrac{\partial}{r\partial\theta} \end{bmatrix}, \quad \boldsymbol{D}_s=\begin{bmatrix} \dfrac{\partial}{\partial r} & 0 & 1 \\ \dfrac{\partial}{r\partial\theta} & -1 & 0 \end{bmatrix}$$

Substituting equations (3) into the following variational function of HMFEM [7] :

$$\pi_R=\sum_e \left\{ \int_{\Omega_e} \left[ -\frac{1}{2}\sigma^T S\sigma+\sigma^T(Du) \right] d\Omega - \int_{S_{\sigma e}} \overline{T}^T u dS-\int_{\Omega_e} \overline{F}^T u d\Omega \right\} \tag{4}$$

where $e$ , $\Omega_e$ , $S$, $S_{\sigma e}$ , $\overline{T}$ and $\overline{F}$ are element numbers, the domain of the element $e$ , elastic compliance matrix, stress boundary, surface force on $S_{\sigma e}$ and body force on element $e$ , respectively.

we obtain variational function of HMFEM for plate bending, as follows:

$$\pi_R=\sum_e \left\{ \int_{\Omega_e} \left[ -\frac{1}{2}M^T S_f M-\frac{1}{2}Q^T S_s Q+M^T(Du)+Q^T(Du) \right] d\Omega-\int_{S_{\sigma e}} \overline{T}^T u dS-\int_{\Omega_e} \overline{F}^T u d\Omega \right\} \tag{5}$$

where

$$S_f=\frac{12}{Et^3}\begin{bmatrix}1 & -\nu & 0\\ -\nu & 1 & 0\\ 0 & 0 & 2(1+\nu)\end{bmatrix},\quad S_s=\frac{2.4(1+\nu)}{Et}\begin{bmatrix}1 & 0\\ 0 & 1\end{bmatrix}$$

In equation (3), displacement $u$ is interpolated in terms of nodal displacement $\lambda$, bending and twisting moment, transverse shear force are expanded in terms of parameters $\beta$, as follows,

$$u=N\lambda\ ,\quad M=P_f\,\beta\ ,\quad Q=P_s\,\beta \tag{6}$$

in which $N$ , $P$ are interpolation function, and function matrix, respectively.

$$\beta=\{\beta_1,\ \beta_2,\ \beta_3,\ \ldots,\ \beta_{11}\}\ ,$$

$$\lambda=\{w_1,\ \psi_{r1},\ \psi_{\theta 1},\ w_2,\ \psi_{r2},\ \psi_{\theta 2},\ \ldots,\ w_4,\ \psi_{r4},\ \psi_{\theta 4}\}$$

Equation (6) is substituted into (5), function $\pi_R$ can be written as,

$$\pi_R=\sum_e\{-\frac{1}{2}\beta^TH_f\,\beta+\beta^TG_f\,\lambda-\frac{1}{2}\beta^TH_s\,\beta+\beta^TG\lambda-W^{(e)T}\lambda\}$$

where $W^{(e)}$ is equal effective nodal force, i.e.,

$$W^{(e)}=\int_{S_{\sigma e}}N^T\bar{T}dS-\int_{\Omega_e}N^T\bar{F}d\Omega\ ,$$

the bending and transverse shear parts of the flexibility matrix $H$ and the bending and transverse shear parts of the leverage matrix $G$ are defined respectively by:

$$H_f=\int_{\Omega_e}P_f^T S_fP_f\ d\Omega\ ,\quad H_s=\int_{\Omega_e}P_s^T S_sP_s\ d\Omega\ ,$$

$$G_f=\int_{\Omega_e}P_f^T(DN)d\Omega\ ,\quad G_s=\int_{\Omega_e}P_s^T(DN)d\Omega$$

The stationary condition of $\pi_R$ yields that

$$\begin{cases}-H\beta+G\lambda=0\\ G^T\beta=W^{(e)}\end{cases} \tag{7}$$

Since $H$ is a positive definite matrix and $H^{-1}$ exists, we solve simultaneous matrix equations (7) and obtain the following equilibrium equation expressed by element stiffness matrix $K^{(e)}=G^TH^{-1}G$ .

$$K^{(e)}\lambda=W^{(e)} \tag{8}$$

3.Numerical Analyses

Based on the formulation of HMFEM described in the previous section, numerical calculations are made for moderately thick/thin circular plates. In most published researches [8-10], a uniformly distributed load over the whole surface or concentrated load at the center of the plate were considered. However, in this study non-axisymmetric loads were analyzed. On the other hand, circular plate bending problem under the uniform tension load in radial direction along the outer boundary and distributed vertical load is carried out, as well.

3.1 Circular plate under partially distributed load

Circular plate subjected to a uniform load $p$ of radius "$R$ ", thickness "$t$ " and clamped in the inner edge ($a=R/3$ ) and in the outer boundary is considered, as shown in Fig.3. Fig.4 shows the uniform division of element for model in the direction of circumference and radius alternately, " × " indicates the distribution of a uniform load.

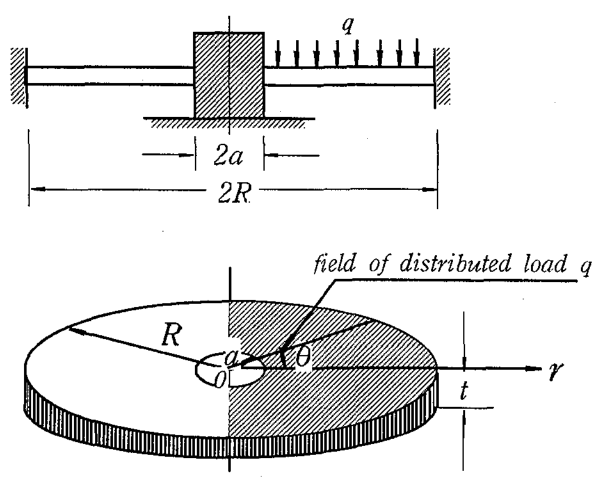


Fig.3 Circular plate

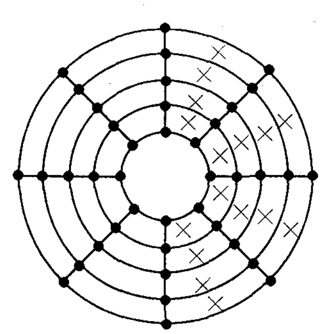

Fig.4 Element division of model

Fig.5 shows the distribution of displacement along radius for the circular plate of $t/R=0.01$ and results compared with theoretical solutions [11]. Numerical results were obtained for adequate convergence by 64 element numbers, as shown in Fig.6. Comparing the results of HMFEM and DFEM shown in Fig.5 and Fig.6 for partial annulus shape element, we conclude that the solutions of the presented method HMFEM(r) (HMFEM under polar coordinate system) are quite close to the classical thin plate solutions and can achieve higher accuracy and faster convergence than DFEM [4] (under Cartesian coordinate system and polar coordinate system, respectively) and HMFEM under Cartesian coordinate system (HMFEM(C)) [4].

In this paper, DFEM expresses displacement finite element method in which a quadrilateral isoparametric displacement finite element and reduced integration technology are used.

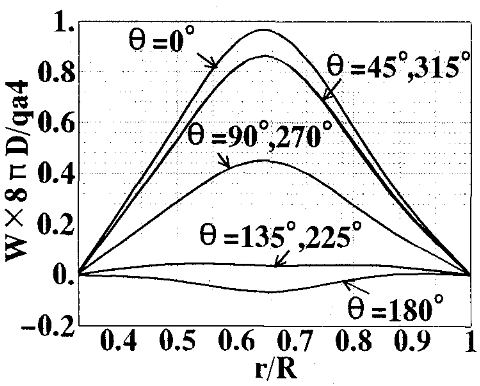


(1) HMFEM

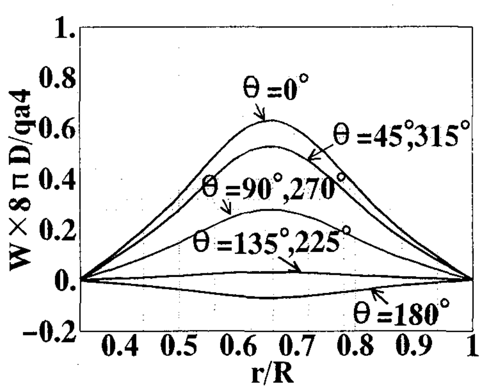


(2) DFEM

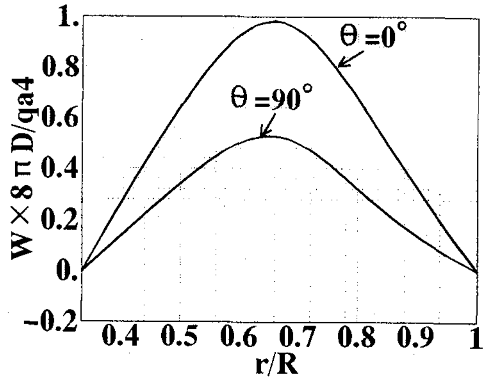


(3) Classical thin plate solution

Fig.5 Distribution of displacement

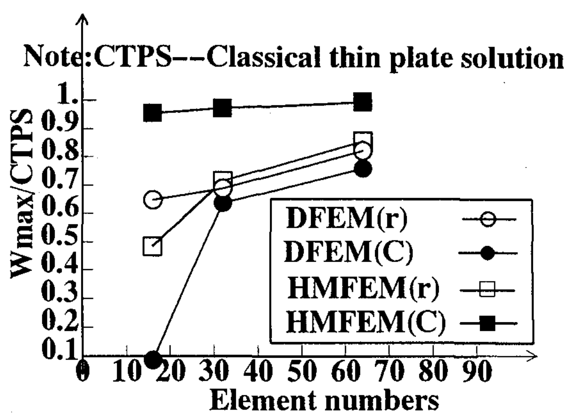


Fig.6 Comparison of solution convergence

Moment $M_r$ is shown in Fig.7, which indicates that the stress of inner boundary along $r=a$ is large and the stress of outer boundary along $r=R$ is comparatively small. It can be see that the results of HMFEM corresponding to $t/R=0.01$ are in close agreement with that of classical thin plate theory. The obvious differences of solutions by DFEM and classical thin plate theory are shown although the affection of the transverse shear deformation is very small when the plate of $t/R=$ $0.01$ is considered.

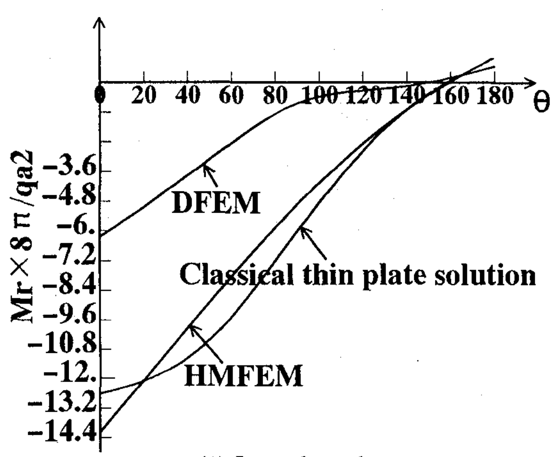


(1) Inner boundary

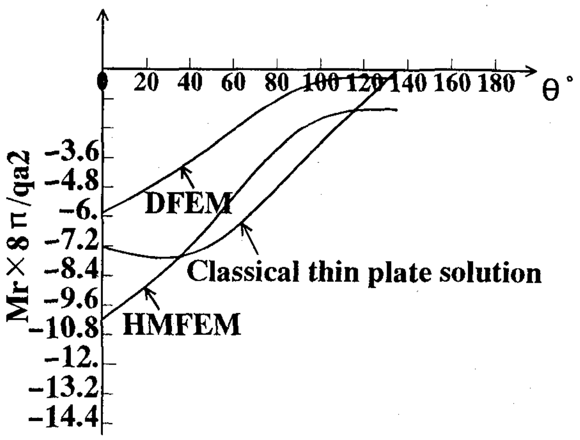


(2) Outer boundary

Fig.7 Distribution of bending moment $M_r$

Table 1 shows the results of the presented method and DFEM in the thin plate limit which the ratio of the plate thickness $t$ and the radius of circular plate $R$ becomes very small. The presented method gives the stable solutions; however, DFEM has "locking" phenomenon. The solutions of plate bending based on Reissner−Mindlin theory different from those of classical thin plate theory when $t/R$ is $0.1$, because transverse shear deformation is considered.

Table 1 Solutions in thin plate limit

| | $W_{max} \times \frac{8\pi D}{qa^4}$ | | $(M_r)_{max} \times \frac{8\pi}{qa^2}$ | |
|---|---|---|---|---|
| *t/R* | *HMFEM* | *DFEM* | *HMFEM* | *DFEM* |
| $10^{-1}$ | 1.0588 | 0.8937 | 12.2542 | 8.4537 |
| *Reference solution: 1.0643* [12] | | | | |
| $10^{-2}$ | 0.9792 | 0.7685 | 12.2454 | 8.7518 |
| $10^{-3}$ | 0.9761 | 0.6099 | 12.2454 | 7.8490 |
| $10^{-4}$ | 0.9761 | 0.5092 | 12.2454 | 5.3222 |
| $10^{-5}$ | 0.9761 | 0.5065 | 12.2454 | 5.2070 |
| $10^{-6}$ | 0.9761 | 0.5065 | 12.2454 | 5.2058 |
| $10^{-7}$ | 0.9761 | 0.5065 | 12.2454 | 5.0077 |
| $10^{-8}$ | 0.9761 | − | 12.2454 | − |
| *Reference solution: 0.988* [10] | | | *12.2554* | |

3.2 Circular plate with inner edge clamped and the outer edge clamped or free

Consider the case of circular plates of clamped along the inner hole and free or clamped along the outer boundary under a concentrated force at distance $r=2R/3$ from the center of the plate, as shown in Fig.8.

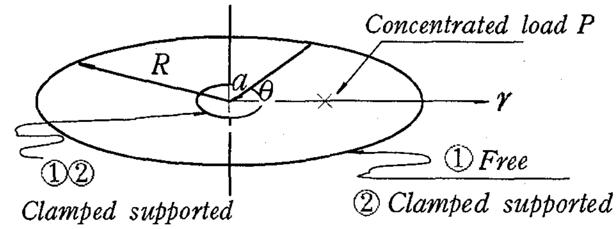


Fig.8 Circular plate under a concentrated load

Fig.9 shows the distributions of moment where the inner edge is clamped and the outer edge is free ( ① ). Comparison of the computational results of HMFEM and DFEM indicate that the distribution is symmetrical along $\theta=0°$ and $\theta=180°$ and the distributions of displacement, rotation displacements $\psi_r$ , $\psi_\theta$ under clamped condition ( ② ) for DFEM, HMFEM and theoretical solution, are shown in Fig.10 and Fig.11, respectively. The results obtained from the presented method are closer to classical thin plate solutions than is DFEM.

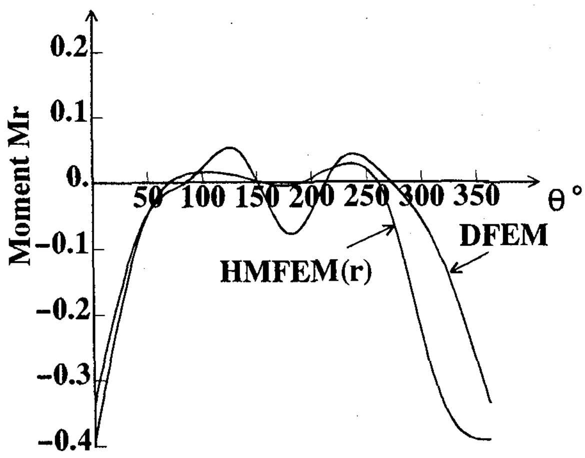


Fig.9 Distribution of moment under free edge

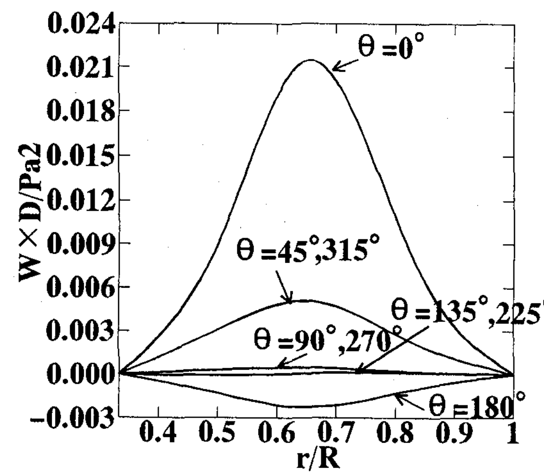


(1) HMFEM(r)

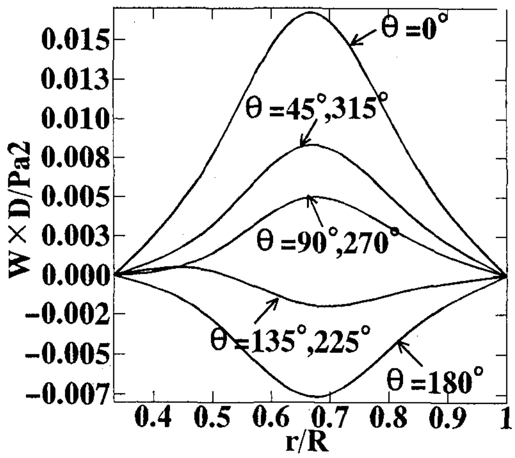


(2) DFEM

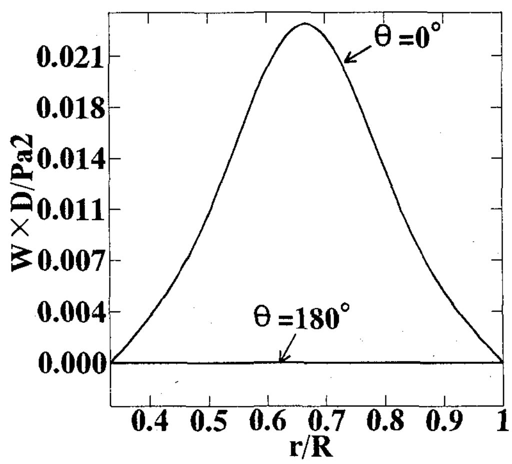


(3) Classical thin plate solution

Fig.10 Distribution of displacement under clamped supported condition

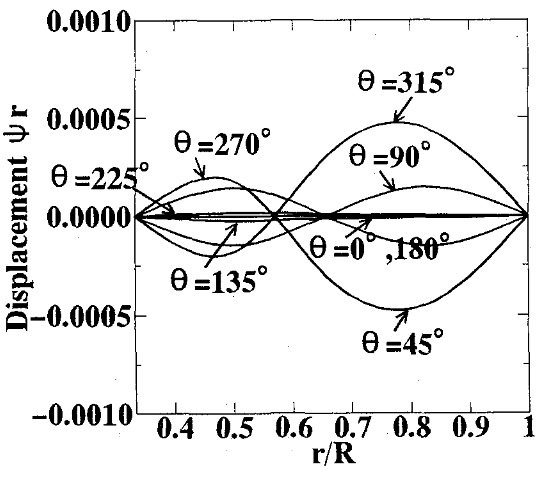


(1)Rotation displacement $\psi_r$

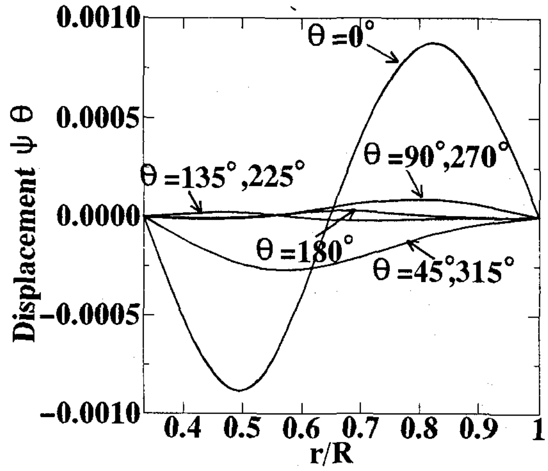


(2)Rotation displacement $\psi_\theta$

Fig.11 Distribution of rotation displacements ($\psi_r$, $\psi_\theta$) under clamped condition

Table 2 shows the results in thin plate limit under the outer edge clamped condition. The results of HMFEM have stability; however, DFEM has the same "locking" phenomenon as the analyses of section 3.2 show.

Table 2 Solutions in thin plate limit

| | $0.01\times W_{max}D/Pa^2$ | | $(M_r)_{max}/P$ | |
|---|---|---|---|---|
| $t/R$ | HMFEM | DFEM | HMFEM | DFEM |
| $10^{-1}$ | 2.77832 | 2.89124 | −0.3945 | −0.3398 |
| $10^{-2}$ | 2.764608 | 2.888489 | −0.3920 | −0.3368 |
| $10^{-3}$ | 2.400842 | 2.871443 | −0.3559 | −0.3363 |
| $10^{-4}$ | 2.393459 | 2.827084 | −0.3554 | −0.3373 |
| $10^{-5}$ | 2.385106 | 2.805984 | −0.3553 | −0.3366 |
| $10^{-6}$ | 2.384202 | 2.805127 | −0.3553 | −0.3366 |
| $10^{-7}$ | 2.308473 | 2.834763 | −0.3587 | −0.3389 |
| $10^{-8}$ | 1.471999 | 0.034175 | −0.2616 | −0.0938 |

3.3 Circular plate under uniform lateral load and uniform tension

The circular plate, which was subjected to a uniform tension $N$ and a distributed uniform load $q$ in vertical plane together simply supported in the outer boundary, is shown in Fig.12. Fig.13 gives a element division of the above model.

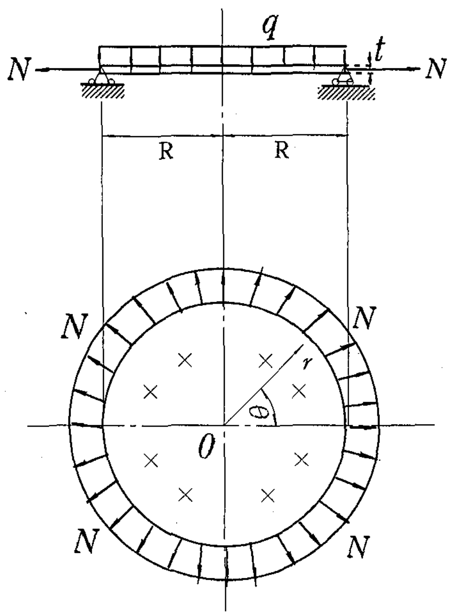


Fig.12 Circular plate under distributed load and uniform tension $(t/R=0.01)$

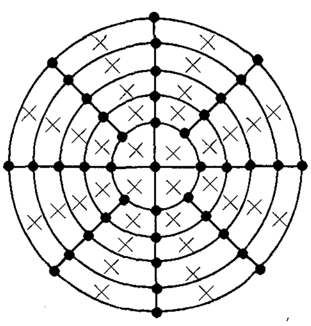

Fig.13 Element division of model

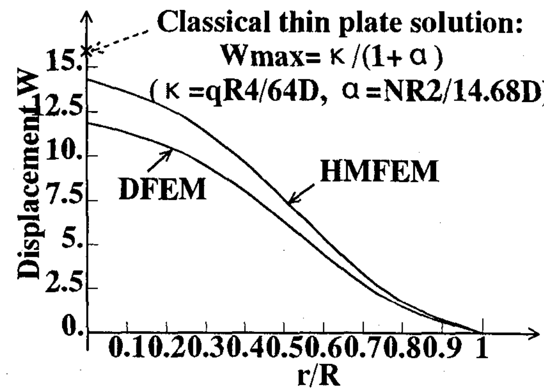


Fig.14 Comparison of maximum displacement under clamped condition

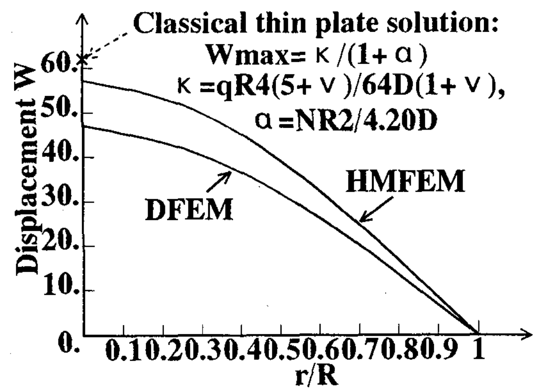


Fig.15 Comparison of maximum displacement under simply supported condition

The theoretical solutions are utilized to compare with the results of the presented analysis and the displacement finite element solution. Fig.14 and Fig.15 describe the distribution of displacement in the direction of radius for $\theta=0^{\circ}$ under clamped and simply supported, respectively. The displacement $W$ reaches a maximum at $r=\theta=0$ . The numerical results show that the results by the presented method yields a higher precise than those by DFEM even a few of element numbers are used. $D$ , $\nu$ which are shown in Fig.14 and Fig.15 are the bending rigidity of the plate and Poisson's ratio, respectively.

4. Conclusions

HMFEM of circular plate bending under polar coordinate system has been proposed in this paper. The formulation of HMFEM is derived based on Reissner−Mindlin plate theory. The convergence of displacement and moments versus the element numbers for moderately thick plate is depicted. It is worth noting that the aspect ratio of plate does not influence the convergence of the results for the presented method. Therefore, HMFEM seems to have a wide applicability to the bending problem of moderately thick plate. By obtaining a model of plate for HMFEM, the bending behaviour of circular plates with non−axisymmetric loads is analyzed. In the preceding examples it is seen that the results of the presented method for both the displacement and the moment are in agreement with classical thin plate solutions in thin plate limit. Therefore, the presented method is a competitive method in terms of efficiency, reliability, accuracy and economy in such applications of circular plate.

References

1) Pian,T.H.H., Derivation of element stiffness matrices by assumed stress distributions, AIAA 7, pp.1333−1335, 1964.
2) Pian, T.H.H., Survey of hybrid/mixed finite element methods for plate and shell analysis, Third Asian−Pacific Conference on Computational Mechanics, pp.

227−232, 1996.
3) Duan, M., Miyamoto, Y., Iwasaki, S., Deto, H. and Zhou, B.K., An efficient six−node plate bending hybrid/mixed element based on Mindlin/Reissner plate theory, Structural Engineering and Mechanics, Vol.5, No.1, pp.69−83, 1997.
4) Duan, M., Miyamoto, Y., Iwasaki, S. and Deto, H., Application of hybrid/mixed plate bending elements in steel structure analysis, Journal of Constructional Steel, Vol.3, pp.185−192, November, 1995. (Japanese)
5) Reissner, E., The effect of transverse shear deformation on the bending of elastic plates", J. Appl. Mech., 12(2), A69−A77, 1945.
6) Mindlin, R.D., Influence of rotatory inertia and shear on flexural motions of isotropic, elastic plates", J. Appl. Mech, 18(1), pp.31−38, 1951.
7) Pian, T. H. H., Chen D. P. and Kang, D., A new formulation of hybrid/mixed finite elements, Comp. and Struct. 16, pp.81−87, 1983.
8) Saleeb, A.F. and Chang, T. Y., An efficient quadrila−teral element for plate bending analysis, Int. J. N. M. E., 24, pp.1123−1155, 1987.
9) Cheung Y.K. and Chen W. J., Refined nonconforming element method for thin plate bending analysis, Third Asian−Pacific Conferece on Computational Mechanics, pp.15−26, 1996.
10) JSCE, The Structural Mechanics Handbook, 1986.
11) Timoshenko, S. P. and Woinowsky−Krieger, S., Theory of Plates and Shells, 2nd ed., McGraw−Hill, 1959.
12) Clive L. D. and Irving H. S., Solid Mechanics: A Variational Approach, McGraw−Hill, Inc. 1973.

(Received September 26, 1997)